

Laboratory Evaluation of a Multi-Array Sensor for Detection of Underdeposit Corrosion and/or Microbially Influenced Corrosion

Michael H. Dorsey
DuPont Engineering Research & Technology
Orange, Texas 77630, USA

Daniel R. Demarco
DuPont Central Research and Development
Environmental & Microbiological Sciences and Engineering
Newark, De 19702

Brian J. Saldanha
DuPont Engineering Research & Technology
Experimental Station
Wilmington, De 19803

George A. Fisher
DuPont Central Research and Development
Environmental & Microbiological Sciences and Engineering
Newark, De 19702

Lietai Yang and Narasi Sridhar
Southwest Research Institute
San Antonio, TX 78238-5166, USA

ABSTRACT

Real-time coupled multielectrode array sensors (MAS) and other monitoring tools were used to evaluate the corrosion of carbon steel and stainless steel in a laboratory based recirculating flow loop simulating an industrial cooling water system. The design and implementation of the monitoring system and results are discussed in this paper. Characterization of the degree and depth of attack from the MAS probe showed good correlation with characterization of underdeposit attack on corrosion coupons that were exposed simultaneously with the MAS probe. In addition, sensor response was altered in the presence of microorganisms suggesting the possible influence of biofilm and/or microbial products on corrosion rates and sensor signals.

Keywords: multielectrode array sensor, coupled multielectrode, corrosion monitoring, cooling water corrosion, localized corrosion, pitting corrosion, MIC, microbially influenced corrosion.

INTRODUCTION

The purpose of the present work was to more fully understand the occurrence of localized corrosion on carbon steel and its possible relationship to microbially influenced corrosion using a coupled multielectrode array sensor and other on-line monitoring tools with standard microbiology techniques. A laboratory based recirculating flow loop was constructed in order to test the response of different electrochemical sensors including the MAS probe and traditional corrosion monitoring tools to the presence of microbial activity and/or biofilm formation. All of the probes were installed in-line in the flow loop. In addition, carbon steel corrosion monitoring coupons were placed in the flow loop. Water from a cooling water pond at a DuPont plant site experiencing severe carbon steel corrosion was used as the test substance. The water is known to contain high levels of microorganisms and therefore microbially influenced corrosion processes are suspected to contribute to the corrosion problem. The probes and coupons were exposed to sterilized (autoclaved) water for 30 days followed by exposure to the same water in the presence of the natural microbial population for an additional 30 days. Data from all probes was collected continuously and coupons were characterized by digital photography, weight loss, and microbiological culture at 30 and 60 days exposures. In addition, water chemistry parameters including pH, ORP, and conductivity were monitored and recorded.

EXPERIMENTAL

Approximately 70 L water from a cooling water pond was added to a recirculating laboratory flow loop containing MAS probes and other water chemistry probes including pH, flow rate, conductivity, and ORP. Water chemistry values were continuously recorded and charted using the Daisy Lab[®] data acquisition software. Culture analysis was carried out by a standard plate count method under aerobic and anaerobic conditions. Briefly, water was diluted in sterile water and 0.1 mL was spread onto Trypticase Soy Agar (TSA) plates and incubated for 3 days at 35°C. Anaerobic incubations were carried out at 35°C for 7 days. Sulfate reducing bacteria (SRB) and iron related bacteria (IRB) testing was performed with the Bart[®] method. Over the course of the study the water was kept at approximately 35°C and was circulated at between 30 and 50 gallons per minute (gpm).

The process water was sterilized by steam sterilization in an autoclave. Following installation of the probes and monitoring coupons the flow loop was “sterilized” by circulation of a 2000 ppm chlorine solution for 30 minutes followed by treatment with non-oxidizing biocide (glutaraldehyde) overnight. A small amount of glutaraldehyde was also added to the water following sterilization to provide additional protection from contamination during the first 30 days of the test. The carbon steel coupons were Type 1018 Carbon Steel (UNS G10180).

Microbiology monitoring as described above was performed on a biweekly basis to ensure system sterility over the first 30 days of the test.

After 30 days the coupons were removed, photographed and cultured. Next, the loop was drained and non-sterile plant cooling water collected from the same location and at the same time as that used for the first 30-day test was added. The test was run for an additional 30 days with the non-sterile water. Monitoring of

water chemistry, probe response, and microbiology was continued. After 30 days the coupons were removed, photographed and cultured.

Online sensors were installed in the test loop to monitor water chemistry as well as two MAS probes. Figure 1 shows the test loop with locations of the various monitoring devices indicated in red. For purposes of this paper only, results from MAS probes and water chemistry, are discussed.

The coupled multielectrode sensor and the high-resolution monitoring system have been described elsewhere¹⁻³. Figure 2 shows typical coupled MAS probes for application in cooling systems. In Figure 2, the sensing electrodes are coupled to simulate a single piece of metal, with some electrodes acting as anodic sites and other electrodes acting as cathodic sites. Each anodic coupling current represents the degree of charge transfer from a corroding (or more corroding) site to a non-corroding (or less corroding) site, which is part of the non-uniform corrosion process. The currents that flow from the anodes (or more anodic electrodes) to the cathodes (or less anodic electrodes) are measured as the corrosion signal. Two of the probes shown in Figure 2 were used in the present study. One of the two probes was a carbon steel (CS) probe and the other was a stainless steel (SS) probe. The sensing electrodes of the CS probe were made of Type 1018 (UNS G10180) wire with a diameter of 4.75×10^{-2} inch (1.21mm); the sensing electrodes of the SS probe were made of Type 316L (UNS S31603) wire with a diameter of 1.1 mm. Both probes have 16 electrodes embedded in an epoxy. Prior to the test, the sensing surface of the probes (the tip of the probe) was polished with 600-grit paper and cleaned with acetone. During the test, only the cross section of the electrodes at the probe tip was exposed to the test solution. The surface area of each electrode was 1.15×10^{-2} cm² for CS probe, and 9.50×10^{-3} cm² for the SS probe. The high-resolution monitoring system measures the localized corrosion rates (pitting or crevice corrosion rates) and the corrosion potentials of the two probes simultaneously. A tungsten/tungsten oxide (W/WO₃) installed in the test loop near the MAS probes was used as the reference probe for the measurements of the corrosion potentials of the MAS probes.

RESULTS AND DISCUSSIONS

Figure 3 shows the localized corrosion (pitting or crevice corrosion) rates of the two MAS probes measured by the MAS system during the 60-day test period. The localized corrosion rate from the carbon steel probe was fairly steady at approximately 2.87 mm/yr (113 mil/yr) during the test with sterile water. However, the localized corrosion rate from the carbon steel probe was fluctuating between 0.56 to 5.3 mm/yr (22.4 to 212 mil/yr) in the non-sterile solution. The average localized corrosion rate from the carbon steel probe during the sterile test was 1.64 mm/yr (64.5 mil/yr). The cumulative depth measured over the 60-day test period for the carbon steel material is 0.37 mm (15 mil). For the stainless steel probe, the localized corrosion rate was low under both the sterile and the non-sterile conditions. The averaged localized corrosion rate from the stainless steel probe was 3.13×10^{-4} mm/yr (1.23×10^{-2} mil/yr) during the whole 60-day test. The cumulative depth measured over the 60-day test for the stainless steel material is 5.2×10^{-5} mm (2.1×10^{-3} mil).

Figure 4 shows the corrosion potential of the two MAS probes measured by the MAS system during the same 60-day test period as shown in Figure 3. The potential of the carbon steel probe was lower than that of the stainless steel probe, suggesting that the carbon steel material was more active than the stainless steel materials in the test solutions. In addition, when the corrosion rate of carbon steel decreased during the test in the non-sterile water, the corrosion potential increased.

Figure 5 shows the appearance of the sensing electrodes of both the carbon steel and stainless steel probes after the 60-day test. Deposits are clearly visible on the electrodes of the carbon steel probe, but not on the stainless steel probe. Figures 6 and 7, show the after-cleaning appearance of the sensing electrodes of the carbon steel and the stainless steel MAS probes respectively. Some of the carbon steel sensing electrodes, were indeed severely corroded, but none of the stainless steel electrodes shows any signs of localized corrosion. The polishing marks on the stainless steel electrodes are clearly visible (Figure 7(b)). It is worth noting that only the electrodes under the deposits (see Figure 5) were severely corroded and the electrodes not covered by the deposits were not corroded after the 60-day exposure in the cooling water system. The corroded electrodes were likely the anodes and the unattacked electrodes were more likely the cathodes during the measurements. The real-time measured low localized corrosion rate from the stainless steel probe and high localized corrosion rate from the carbon steel probe as shown in Figure 3 are in good agreement with the degree of corrosion attack as shown in Figures 6 and 7.

Figure 8 presents the deepest depth of the pits on the sensing electrodes of the carbon steel probe. The depth was from not detectable (N/A) to a maximum of 0.04 in (40 mils). As the MAS technology measures the deepest localized corrosion attack^{1,2}, the depth from the MAS system 0.015 in (1.5 mils) should correspond to the depth of electrode #5 in Figure 8. The slightly lower rate measured by the MAS system is probably due to the non-uniform attack on the electrode (Figure 6(b)). The MAS system calculated the depth by assuming the metal on the small area of the electrode was uniformly corroded. Figure 6(b) shows that only 60% of the small area was corroded but the other 40% was not corroded. Even within the 60% of the corroded area, the corrosion was not uniform either. The MAS concept calls for using small and a large number of electrodes to predict localized corrosion rate. However, in practice, size and the number of the electrodes in a MAS probe is limited by availability of materials and the cost. Figures 3 and 8, show that the carbon steel probe, with 16 electrodes made of 1.21-mm-diameter wires, was able to measure the localized corrosion rate with a factor of 2 to 3 error. This precision is very good considering the difficulties in the measurement of localized penetration rates, which often vary by orders of magnitude.

Figures 9 and 10, show the appearance of the carbon steel coupons before- and after-cleaning after 30 days exposure to the sterile and non-sterile waters, respectively. The severe localized corrosion attack observed under the deposits in Figure 9 is in agreement with the localized corrosion attacks as shown in Figure 7. Similarly to the real-time measured corrosion rates from the carbon steel MAS probe (Figure 3), Figures 9 and 10 also show that localized corrosion attack was more severe in the sterile water than in the non-sterile water.

Table 1 shows the corrosion rates for uniform corrosion obtained with the weight-loss method and the cell counts (TVC; total viable counts) of some of the microbes. Tables 1 and Figures 3, 9 and 10 seem to suggest that the presence of microorganisms over the second half of the test actually acted to protect the carbon steel surfaces from attack and reduce the overall corrosion rate. The presence of large numbers of *Pseudomonas* sp. in the water was confirmed by culture and 16srRNA analysis. It is known that many slime forming bacteria like *Pseudomonas* can form protective biofilms on metal surfaces and act to reduce corrosion attack⁴. Compared with the results in the sterile water, the real-time measured corrosion rate for carbon steel sterile fluctuated significantly in the non-sterile water. It is not known what caused such fluctuations in the non-sterile water. It should be noted that the corrosion rates presented in Table 1 corresponds to the uniform corrosion rate. The depth of localized attack in similar coupons under-deposit corroded areas have showed depths of attack that were 5-10x of the general corrosion rates¹, which translates to localized under-deposit corrosion rates of 100-200 mpy.

Figures 11 through 14 show the flow rate and water chemistry of the loop. There was no significant trend for the flow rates. The conductivity increased gradually from 700 to 820 μS during the sterile test and approximately 800 μS during the non-sterile test. The pH decreased gradually from 8.8 to 7.8 during the sterile test and fluctuated between 7.4 and 8 during the non-sterile test. The ORP (Oxidation and reduction potential on platinum electrode) in the non-sterile water was significantly higher than that in the sterile water. It is difficult to correlate the corrosion rate as shown in Figure 3 with these bulk water chemistries.

CONCLUSION

The corrosion behavior of carbon steel and stainless steel materials under deposits were investigated in a recirculating flow loop simulating the cooling water system in a chemical plant. Coupled multielectrode array sensors and other online monitoring tools were used in the studies. Coupons were also installed in the test loop for comparison with the online measured corrosion rate results. The results show that the localized corrosion rate from the carbon steel MAS probe was in good agreement with the actual depth measurements of the localized corrosion attack on the sensing electrodes of the probe and the surface of the test coupons.

ACKNOWLEDGMENTS

The authors acknowledge the assistance of Julio Ramirez, David Huntley, and Mike Monack (DuPont Co.) for their assistance in the construction of the laboratory flow loop and setup of data acquisition software.

REFERENCES

1. M.H. Dorsey, Lietai Yang and Narasi Sridhar, Cooling Water Monitoring Using Coupled Multielectrode Array Sensors and Other On line Tools, Michael CORROSION/2004, paper no. 04077, Houston, TX: NACE International, 2004.
2. Lietai Yang and Narasi Sridhar "Coupled Multielectrode Online Corrosion Sensor", Materials Performance, Vol. 42, No. 9, pp. 48-52, 2003.
3. L. Yang, N. Sridhar, O. Pensado, and D. S. Dunn, "An In-situ Galvanically Coupled Multielectrode Array Sensor for Localized Corrosion", Corrosion, 58, 1004, 2002.
4. B. Little and R. Ray, "A Perspective on Corrosion Inhibition by Biofilms", Corrosion 58, 5 (2002): p. 424.

Table 1. Uniform Corrosion rate and microbiology measurements - carbon steel coupons

| Coupon Type and Number | Exposure Time/Conditions | Corrosion Rate (mpy) | TVC Aerobic (CFU/cm²) | TVC Anaerobic (CFU/cm²) | IRB (CFU/cm²) | SRB (CFU/cm²) |
|-------------------------------|---------------------------------|-----------------------------|---|---|---------------------------------|---------------------------------|
| CS #1 | 30 day sterile site water | 20.61 | N.M. | N.M. | N.M. | N.M. |
| CS #2 | 30 day sterile site water | 22.34 | N.M. | N.M. | N.M. | N.M. |
| CS #3 | 30 day sterile site water | 19.05 | N.M. | N.M. | N.M. | N.M. |
| CS #4 | 30 day sterile site water | 24.87 | N.M. | N.M. | N.M. | N.M. |
| CS#5 | 30 day non-sterile site water | 1.15 | 5.00E+03 | 6.00E+01 | N.D. | N.D. |
| CS#6 | 30 day non-sterile site water | 1.26 | 2.50E+03 | 1.00E+01 | N.D. | N.D. |
| CS#7 | 30 day non-sterile site water | N.M. | N.M. | N.M. | N.M. | N.M. |
| CS#8 | 30 day non-sterile site water | N.M. | N.M. | N.M. | N.M. | N.M. |

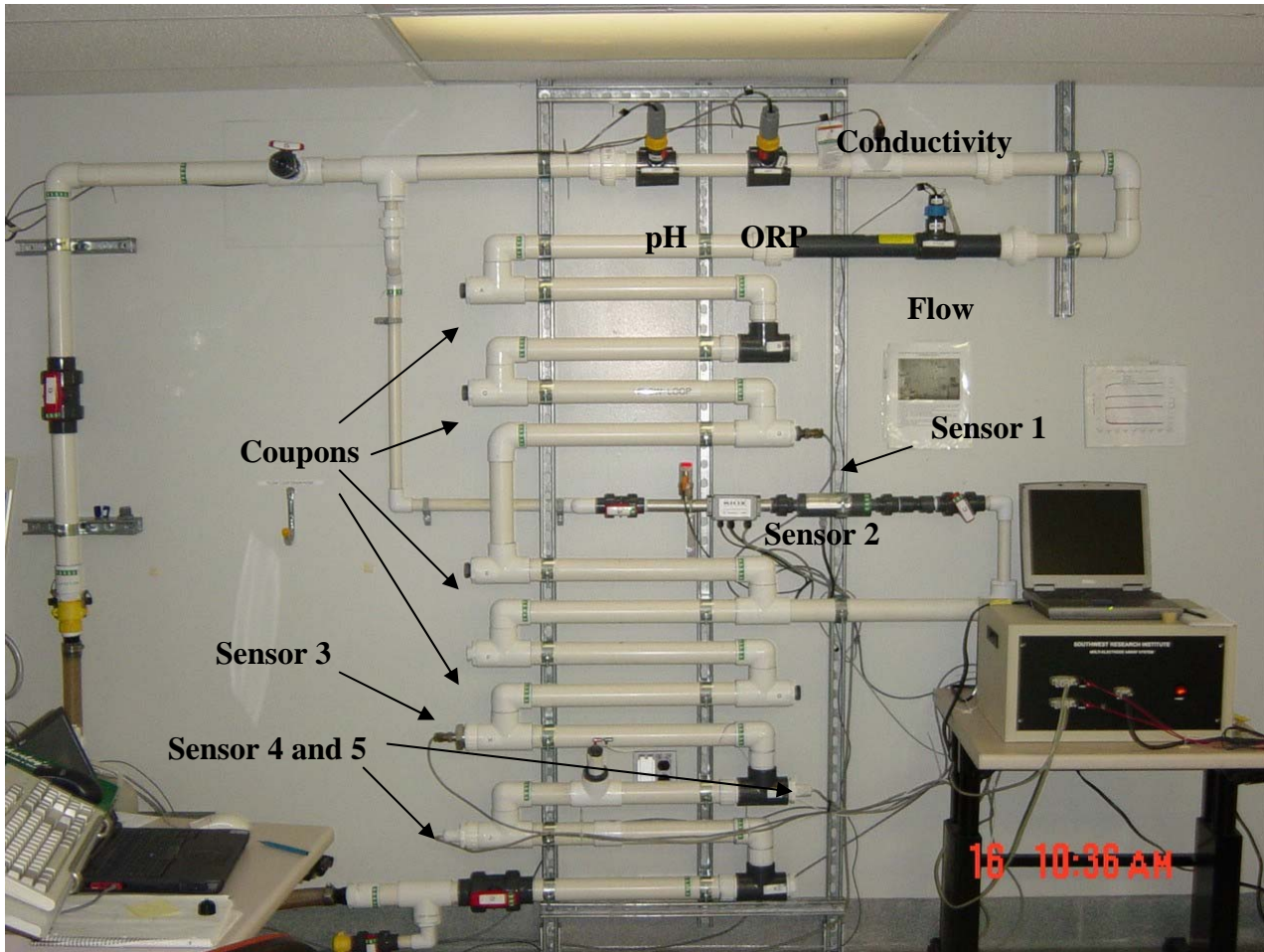
TVC = total viable counts

IRB = iron related bacteria

SRB = sulfate reducing bacteria

N.D. = none detected, <10 CFU/ml

N.M. = not measured



Sensor 1 = BioGeorge probe
Sensor 2 = BIOX probe
Sensor 3 = BioGeorge probe
Sensor 4 and 5 = MAS probes

Figure 1. Laboratory Flow Loop



Figure 2. Typical 16-electrode MAS probes used in the experiment

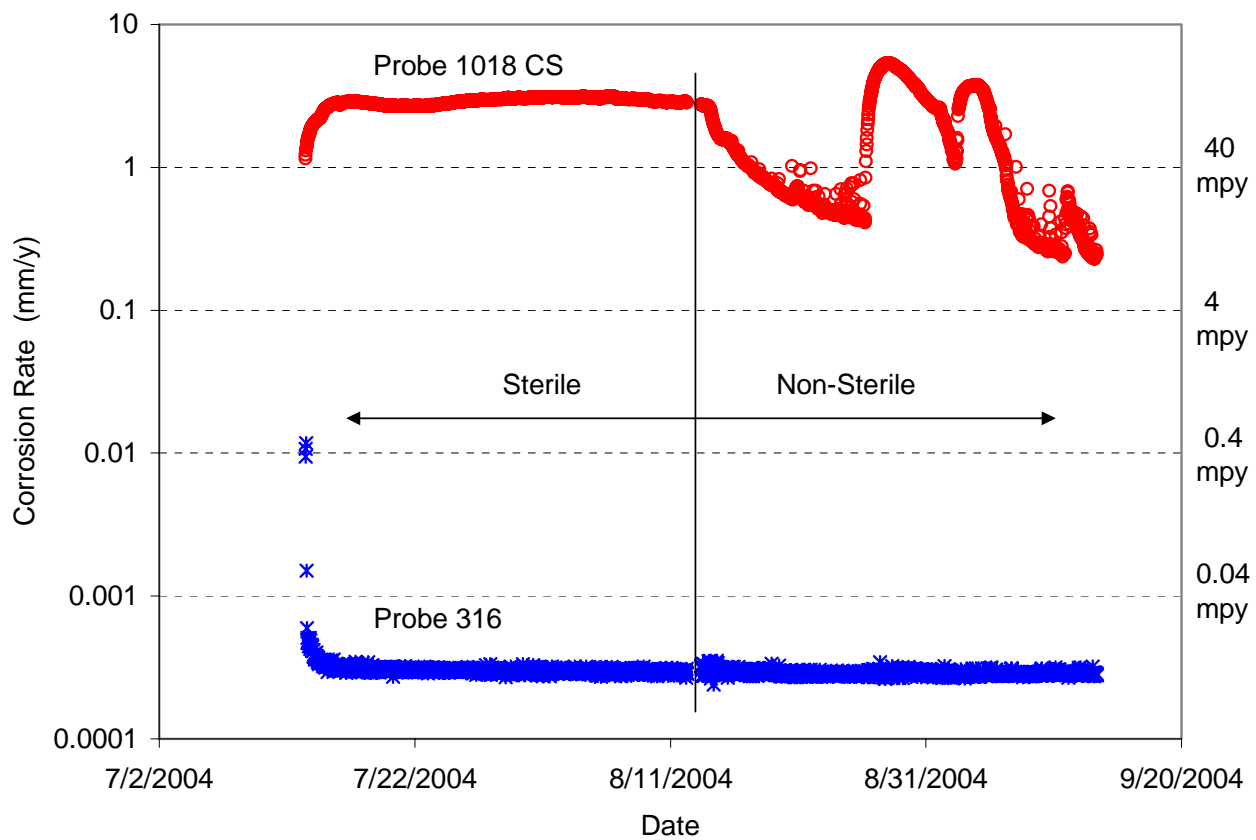


Figure 3. Localized Corrosion rates measured from the Type 1018 carbon steel and Type 316L stainless steel probes during the 60-day tests

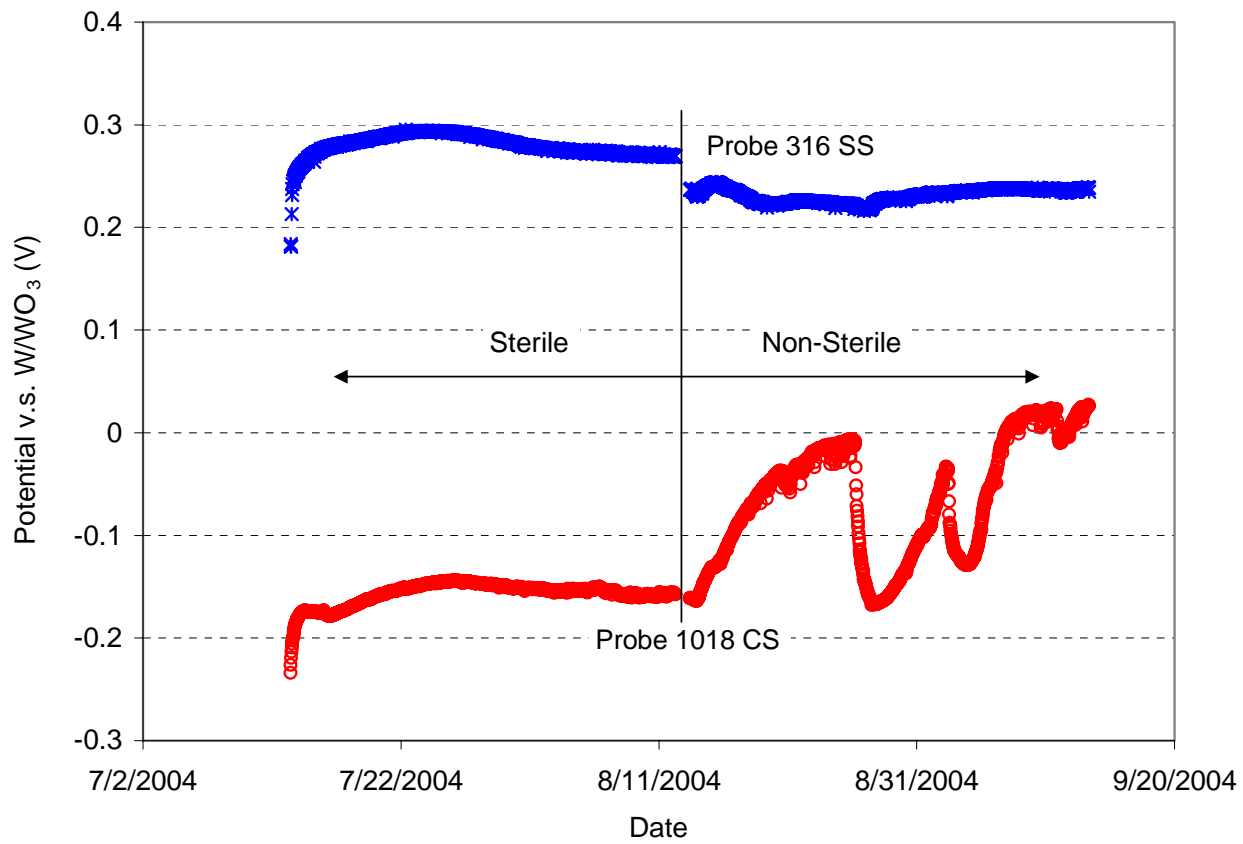


Figure 4. Corrosion potential measured from the Type 1018 carbon steel and Type 316L stainless steel probes during the 60-day test

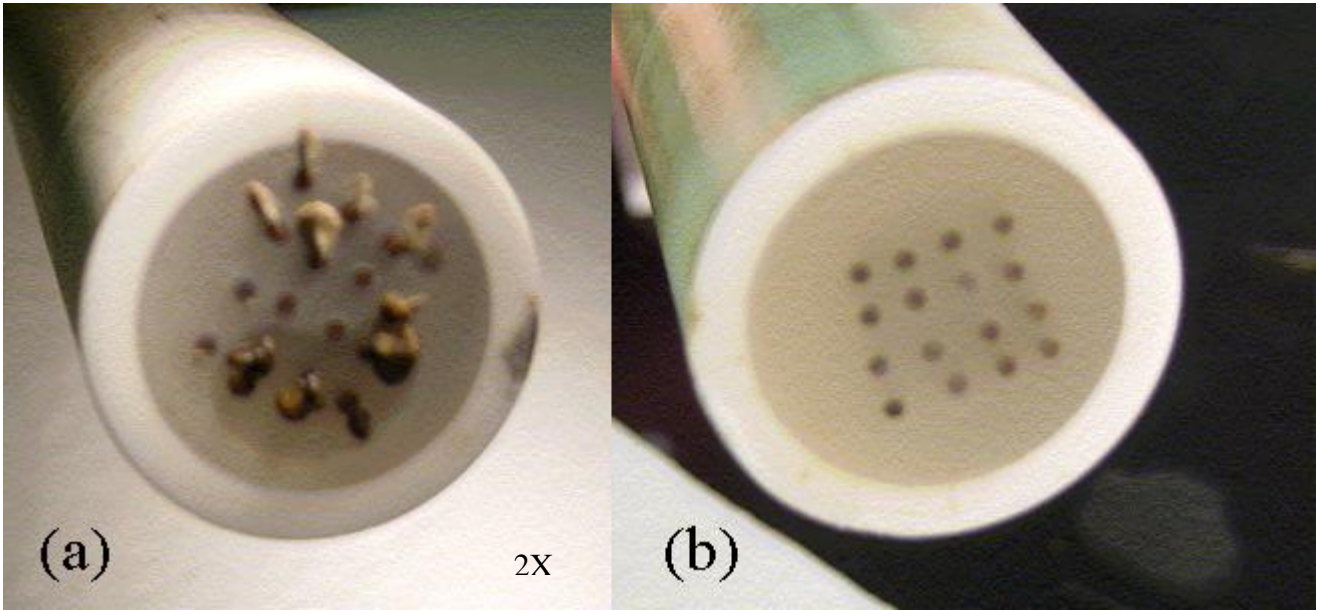


Figure 5. Appearance of the carbon steel (a) and stainless steel (b) probes after the 60-day test

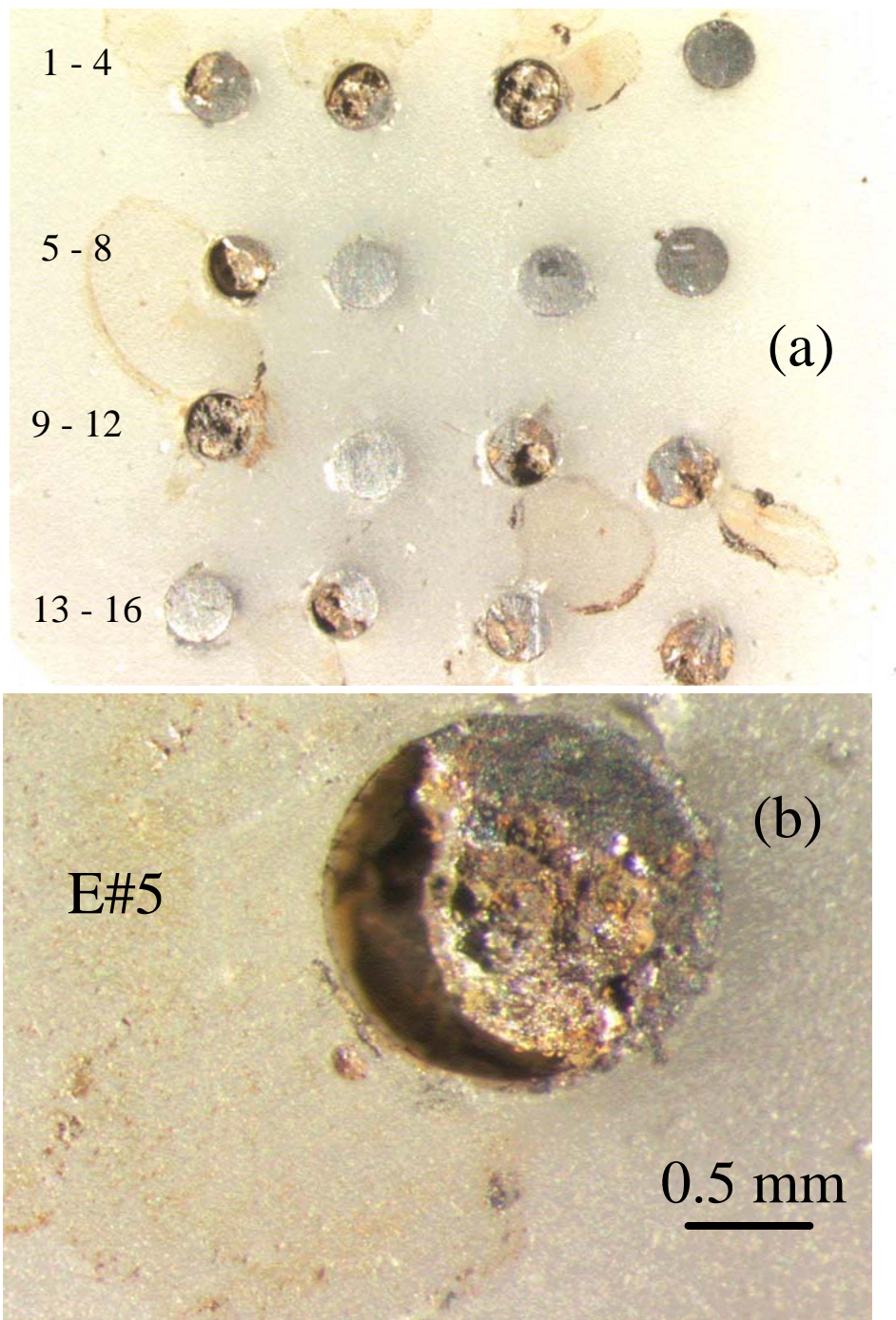


Figure 6. After-cleaning appearance of the carbon steel MAS probe electrodes (a) and the pit developed on electrode # 5 (b) after 60-day exposure

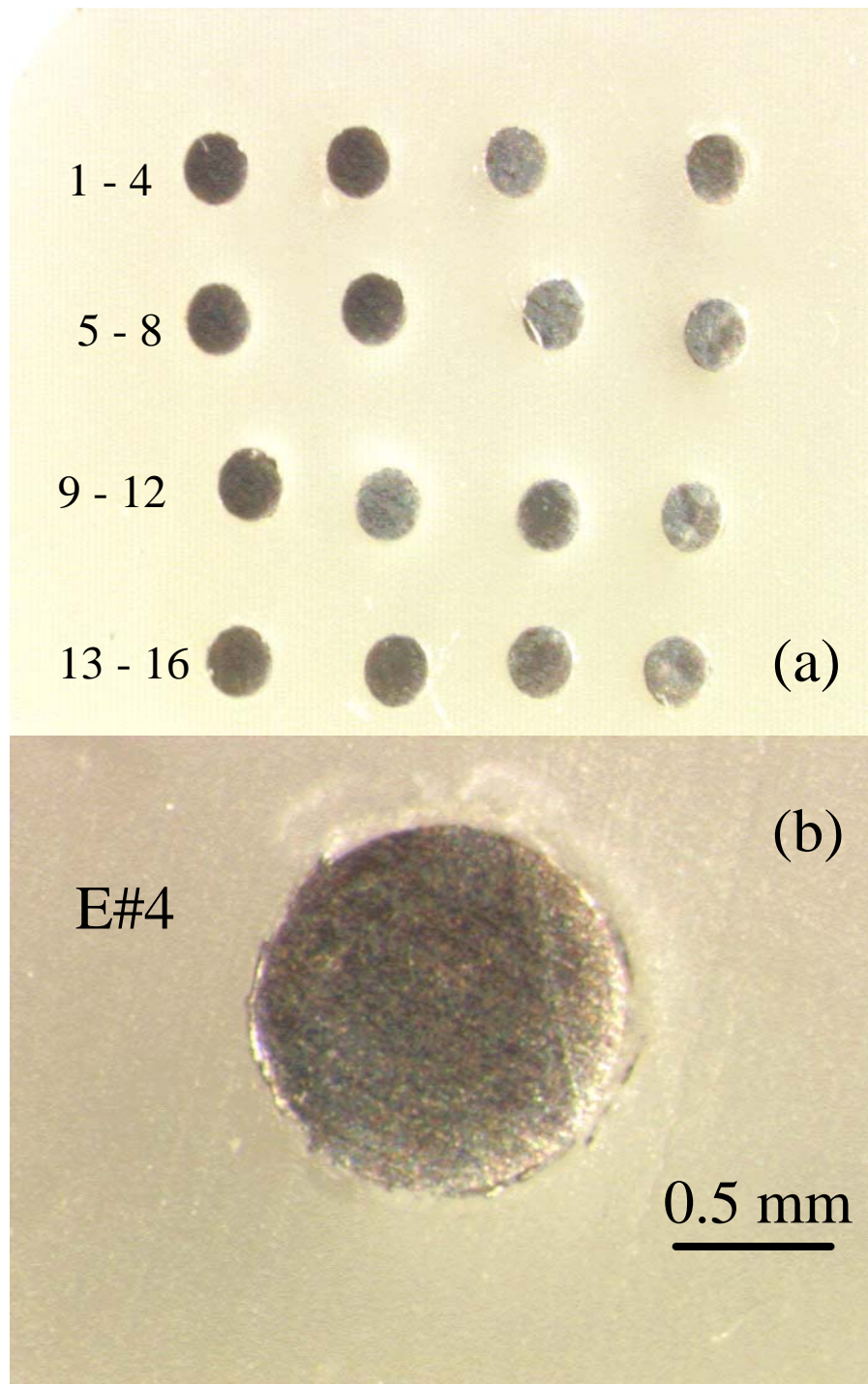


Figure 7. After-cleaning appearance of the stainless steel MAS probe electrodes (a) and the enlarged view of electrode # 4 (b) after 60-day exposure

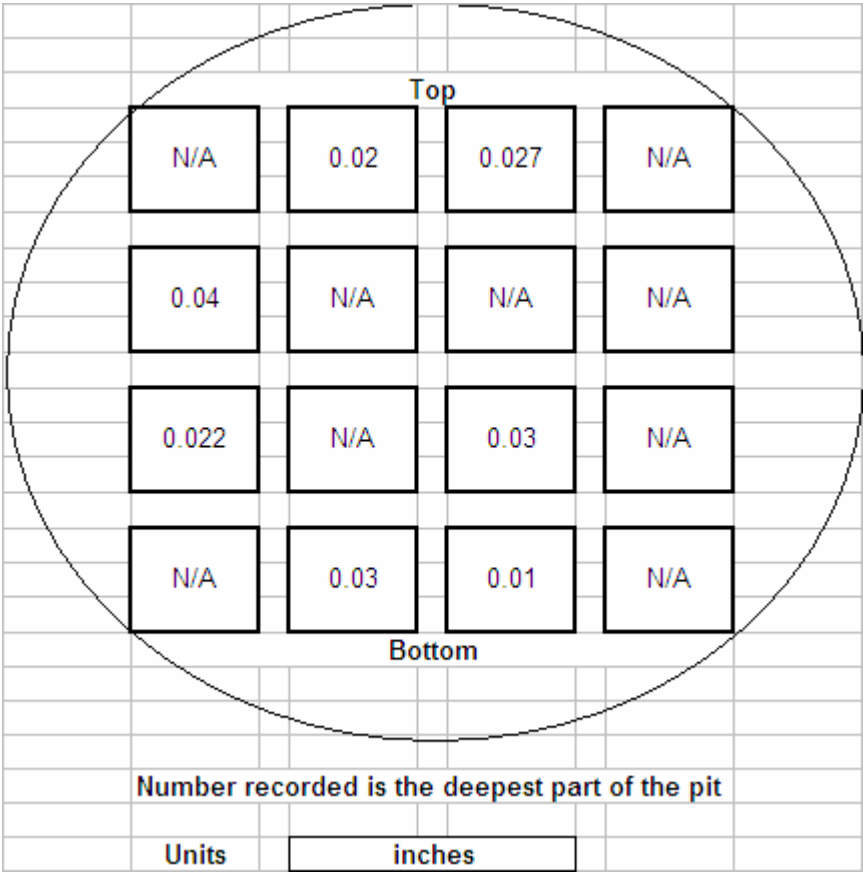


Figure 8. Depth of pitting attack (inches) on the carbon steel electrodes as shown in Figure 6(a).

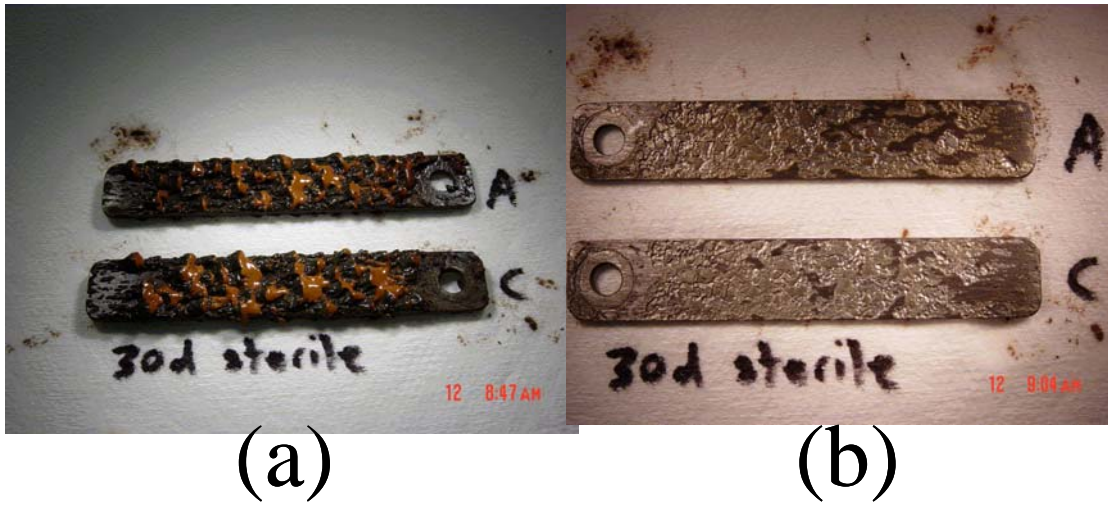


Figure 9. Appearance of typical carbon steel coupons at the end of the 30-day exposure in sterile water (a) before and (b) after cleaning .

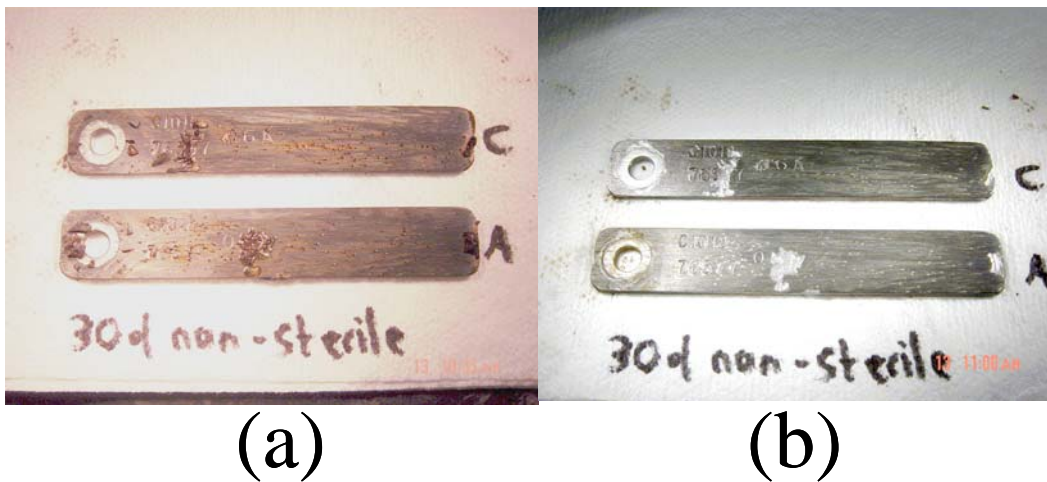


Figure 10. Appearance of typical carbon steel coupons at the end of the 30-day exposure in non-sterile water (a) before and (b) after cleaning.

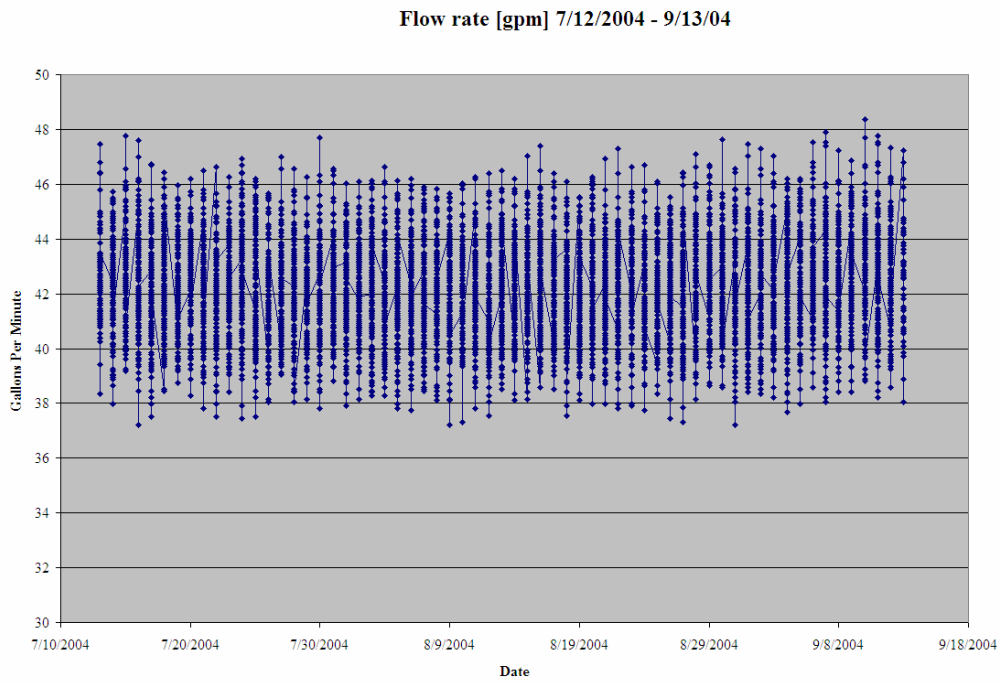


Figure 11. Water chemistry data – flow rate

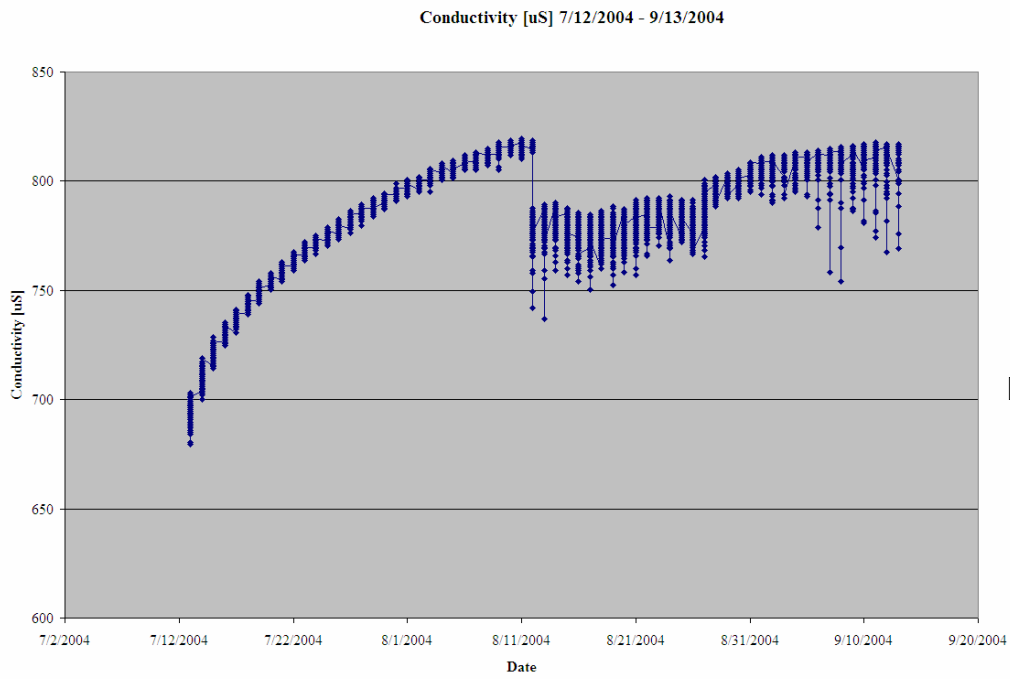


Figure 12. Water chemistry data - conductivity

pH [pH] 7/12/2004 - 9/13/04

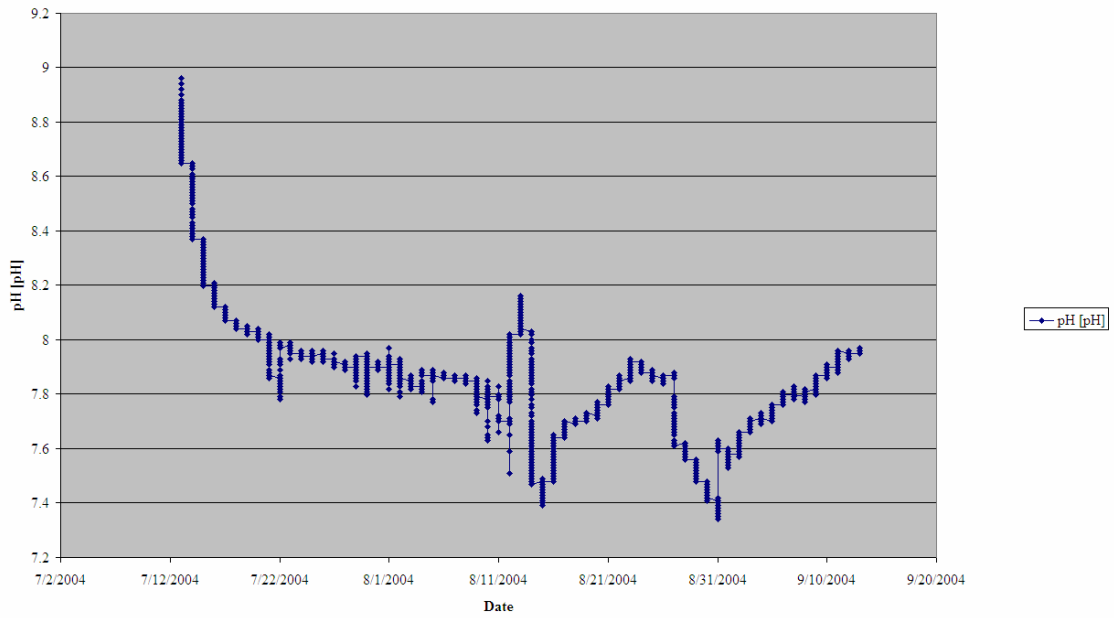


Figure 13. Water chemistry data - pH

ORP [mV] 7/12/2004 - 9/13/04 - (30 Day Sterile)

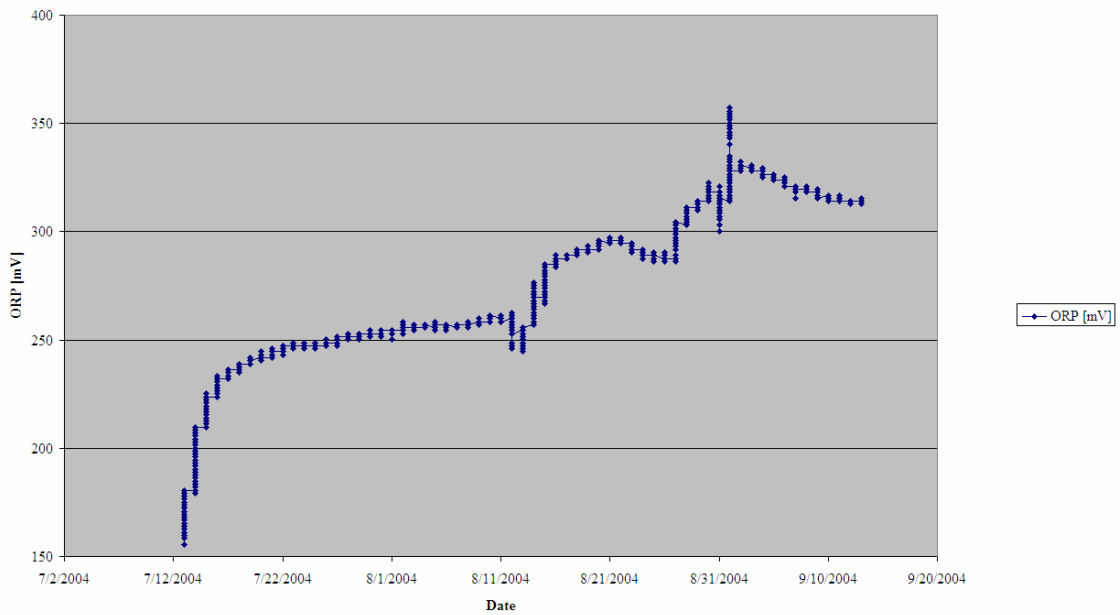


Figure 14. Water Chemistry Data - ORP